

1 Development of a microscale land use regression model for predicting NO<sub>2</sub> concentrations at  
2 a heavy trafficked suburban area in Auckland, NZ

3

4 Weissert, LF<sup>1)</sup>, Salmond, JA<sup>2)\*</sup>, Miskell, G<sup>1)</sup>, Alavi-Shoshtari, M<sup>1)</sup>, Williams, DE<sup>1)</sup>

5

6 <sup>1)</sup> School of Chemical Sciences, Faculty of Science, University of Auckland, New Zealand

7 <sup>2)</sup> School of Environment, Faculty of Science, University of Auckland, Auckland, New Zealand

8

9 \* Corresponding author. E-mail address: j.salmond@auckland.ac.nz, Tel:+64 9 3737599 ext

10 88650

11

12

13

14 Abstract

15 Land use regression (LUR) analysis has become a key method to explain air pollutant  
16 concentrations at unmeasured sites at city or country scales, but little is known about the  
17 applicability of LUR at microscales. We present a microscale LUR model developed for a  
18 heavy trafficked section of road in Auckland, New Zealand. We also test the within-city  
19 transferability of LUR models developed at different spatial scales (local scale and city scale).  
20 Nitrogen dioxide (NO<sub>2</sub>) was measured during summer at 40 sites and a LUR model was  
21 developed based on standard criteria. The results showed that LUR models are able to capture  
22 the microscale variability with the model explaining 66% of the variability in NO<sub>2</sub>  
23 concentrations. Predictor variables identified at this scale were street width, distance to major  
24 road, presence of awnings and number of bus stops, with the latter three also being important  
25 determinants at the local scale. This highlights the importance of street and building  
26 configurations for individual exposure at the street level. However, within-city transferability  
27 was limited with the number of bus stops being the only significant predictor variable at all  
28 spatial scales and locations tested, indicating the strong influence of diesel emissions related to  
29 bus traffic. These findings show that air quality monitoring is necessary at a high spatial density  
30 within cities in capturing small-scale variability in NO<sub>2</sub> concentrations at the street level and  
31 assessing individual exposure to traffic related air pollutants.

32

33 Keywords: LUR; air pollution; nitrogen dioxide; intra-urban air pollution; transferability;

34 GIS

35 Introduction

36 In many cities, personal exposure to air pollution is primarily determined by time spent in the  
37 transport micro-environment (Dirks et al., 2012; McNabola et al., 2009; Kaur and  
38 Nieuwenhuijsen, 2009). However, time spent in this environment is not limited to commuter  
39 activities, and high densities of people are also observed moving through transport corridors as  
40 they visit the shops, restaurants and recreational facilities found clustered along busy streets  
41 and intersections. In such transport micro-environments the temporal and spatial variability in  
42 air pollution concentrations is large, and may be even greater than variability between cities  
43 (Hoek et al., 2008; Gurung et al., 2017).

44 Measuring air pollutant concentrations at local (representative of a neighbourhood or suburb)  
45 or microscales (representative of individual roads) in transport corridors is especially  
46 challenging as pollutant concentrations are strongly dependent on short-term traffic conditions  
47 and the configurations of buildings and streets (Eeftens et al., 2013; Miskell et al., 2015). For  
48 example, significant reductions in pollutant concentrations can be observed just a few meters  
49 from emission sources (Grange et al., 2014), and roadside concentrations can differ  
50 substantially from local background concentrations (Vardoulakis et al., 2011). Further,  
51 buildings modify local air flow patterns causing trapping and re-circulatory flows at some  
52 locations and increased dispersion of air pollutants at other locations (Salmond and McKendry,  
53 2009; Salmond et al., 2013; Shi et al., 2016). As a result little is known about the relative  
54 importance of urban morphology, building design, traffic management and infrastructure  
55 (including phasing of traffic lights), and other details such as vegetation or bus stop positions  
56 in determining microscale air quality variability. There is therefore a need to improve our  
57 understanding about the microscale spatial variability of air pollutants in urban hotspots if we  
58 are to develop urban planning and design tools to control and mitigate personal exposure to air

59 pollution in transport corridors, especially at locations where traffic as well as pedestrian  
60 activity is high (Borge et al., 2016).

61 Land use regression (LUR) analysis which emerged as a popular method in epidemiological  
62 studies to predict air pollutant concentrations and assess individual exposure levels (Hoek et  
63 al., 2008; Jerrett et al., 2005). It has the potential to assist urban planners in identifying the key  
64 controls on local air quality in transport corridors. Based on selected land use characteristics  
65 (e.g. distance to nearest road, land cover or population density), which are now widely available  
66 through geographic information (GIS) systems, LUR models allow estimation of air pollutant  
67 concentrations at unmeasured sites based on regression analysis (Hoek et al., 2008; Jerrett et  
68 al., 2005). Thus, LUR models are often used to complement regulatory monitoring networks,  
69 which are usually sparse due to logistical and financial constraints (Hoek et al., 2008;  
70 Vardoulakis et al., 2011). Such models have been primarily developed and applied to urban  
71 scale analyses ( $10^4$  -  $10^5$  m), with some applied to the regional or country scale where they  
72 have been effectively used to identify common determinants of air quality for primarily  
73 transport related pollutants such as nitrogen dioxide (NO<sub>2</sub>). These include factors such as road  
74 length, distance to major roads, land cover, traffic volume and density, population density and  
75 altitude guide Hoek et al. (2008). Final models typically explain around 60 - 70% of the  
76 variability (Beelen et al., 2013) with a range from 51% (Briggs et al., 2000; Gurung et al.,  
77 2017; Morgenstern et al., 2007) to 97% (Stedman et al., 1997).

78 However, there is little evidence to demonstrate their effectiveness (or otherwise) under the  
79 highly heterogeneous conditions typical of multi-use transport corridors, and their ability to  
80 capture and effectively represent local variability at urban hotspots may be limited (Apte et al.,  
81 2017; Ghassoun et al., 2015; Hoek et al., 2008). Further, although LUR models have been used  
82 in numerous cities across Europe and North America (Hoek et al., 2008), results from other  
83 geographical regions have only recently become available and remain limited (e.g. Australia

84 (Dirgawati et al., 2015); China (Meng et al., 2015); Nepal (Gurung et al., 2017); New Zealand  
85 (Miskell et al., 2015); Iran (Amini et al., 2016)).

86 In this study, we present a LUR model developed for urban microscales and applied to a heavily  
87 trafficked suburban street in Auckland, New Zealand. Our study is one of a limited number of  
88 studies (such as Miskell et al., 2015) which address local to microscale spatial variability (1-3  
89 km) and use local urban design features as predictor variables (such as presence or absence of  
90 shop awnings) rather than standard landuse predictors (such as population and household  
91 density) which were homogenous within our study area. In particular, we were interested in  
92 examining the transferability of this approach. We also tested the within-city transferability of  
93 previously developed LUR models and explored the potential to extend the multi-scale model  
94 developed in Auckland's CBD by Miskell et al. (2015) to all spatial scales and sites outside the  
95 CBD. This study therefore also offers new insights into the applicability of LUR models  
96 developed for a certain area to other locations within the same city at different scales, which  
97 has not previously been explored.

98

## 99 Material and Methods

### 100 Study area

101 Auckland is New Zealand's largest and fastest growing city with around 1.5 million inhabitants  
102 (Statistics New Zealand, 2013). Vehicle emissions are the largest contributor to air pollution  
103 in Auckland with traffic-related NO<sub>x</sub> (NO<sub>2</sub>, NO) emissions accounting for almost 80% of the  
104 total NO<sub>x</sub> emissions (Xie et al., 2016). However, pollutants are often dispersed by maritime  
105 winds, which occur year-round favoured by Auckland's location on a narrow isthmus  
106 (Chappell, 2014; Senaratne and Shooter, 2004). The focus of this study was on a heavy  
107 trafficked road (Dominion Road) about 4 km south of the city center (Fig. 1). Dominion Road  
108 is a main route for buses and commuters in and out of the city as well as to the main airport

109 (Auckland Transport, 2017). The area is also well used by pedestrians visiting shops, bars and  
110 cafés along the road, making this an interesting area for air pollution measurements due to the  
111 high traffic and potential exposure.

112



113

114 Fig. 1 Study sites.

115

116 NO<sub>2</sub> concentration measurements

117 NO<sub>2</sub> concentrations were measured by Palmes diffusion tubes at 40 sites along a 2 km section  
118 of Dominion Road (Fig 1). Sites were chosen to reflect a range of urban design features (such  
119 as the presence of building awnings, proximity to bus stops, greenspace, trees and carparks  
120 etc.). Sites were also chosen to represent the range of expected spatial variability of air pollution  
121 concentrations. The number of sites previous other LUR studies ranged from 14 – 107 (see  
122 Hoek et al. 2008, Beelen et al. 2013), with sample sizes of 40 commonly used in the ESCAPE

123 project (which is most commonly referenced as the standard methodology for such studies)  
124 (Beelen et al., 2013). Given the size of our sample area, and the number of different  
125 environments expected, the choice of a sample size of 40 was deemed sufficient and  
126 representative within the context of the resources available.

127 At each site, we deployed two tubes at a height of approx. 2.5 m for four periods of 14 days  
128 between the 18<sup>th</sup> of November 2016 and the 1<sup>st</sup> of February 2017. To assess the reliability of  
129 the NO<sub>2</sub> measurements during each campaign we used travel and laboratory blanks (AEA  
130 Energy and Environment, 2008). Palmes tubes were analysed using a spectrophotometer and  
131 NO<sub>2</sub> concentrations calculated following standard methodology (AEA Energy and  
132 Environment, 2008). The coefficient of variance (CoV) was used to test the agreement between  
133 duplicate readings at each site and results that exceeded a CoV of 0.25 were excluded from the  
134 further analysis (Miskell et al., 2015; Mölter et al., 2012). As there was no reference regulatory  
135 air quality station near the road section studied here, we were not able to apply a seasonal  
136 adjustment to the NO<sub>2</sub> concentrations. Thus, we used seasonally averaged NO<sub>2</sub> concentrations,  
137 representative of typical summer conditions in this study, which are likely slightly below the  
138 annual average. For comparison, NO<sub>2</sub> measured by routine air quality monitors from 2010 –  
139 2011 by the Auckland Council at another urban road (Khyber Pass, approx. 2 km northeast  
140 from Dominion Road) was on average 1 and 3 µg m<sup>-3</sup> below the annual average in December  
141 and January, respectively. Slightly larger differences were observed in Auckland's Central  
142 Business District (CBD) where five-year average NO<sub>2</sub> concentrations measured in December  
143 and January were around 10 µg m<sup>-3</sup> below the annual average (Miskell, 2013).

144

145 Predictor variables

146 Predictor variables for the initial stages were chosen based on a previous study undertaken in  
147 Auckland (Table 1, (Miskell et al., 2015)) and generated for each site using GIS shape files

148 (Auckland Council, 2013-2014) and aerial photographs. Each variable was either  
149 representative of a pollution source, such as number of lanes, or dispersion modifier, such as  
150 presence of building awnings (Table 1). As traffic density was not available at this high spatial  
151 resolution we used average weekday traffic congestion during the morning rush hour (06:00 –  
152 09:00), midday (11:00 – 13:00) and evening rush hour (17:00 – 19:00) reported on Google  
153 Maps as a proxy. In this area land use, population density, household density and number of  
154 buildings show no significant spatial variability thus these predictors are not included in our  
155 analysis.

156 Table 1. Predictor variables with defined buffer sizes and expected direction of effect.  
157 (Attached at the end of the manuscript)

158

159 LUR model development

160 The LUR model was developed based on stepwise variable selection as outlined by the  
161 ESCAPE protocol (Beelen et al., 2013; Brunekreef, 2008). First, each predictor variable was  
162 compared to the average NO<sub>2</sub> concentrations measured throughout the study period using  
163 univariate regressions. Variables that did not follow the expected slope direction (e.g. an  
164 increase in number of traffic lanes is expected to increase air pollutants) were removed from  
165 further analysis. The variable with the highest adjusted  $R^2$  was used to start developing the  
166 LUR model and predictor variables were then added one at the time and included in the model  
167 following standard procedures of the ESCAPE protocol (Brunekreef, 2008). In the final stage,  
168 variables with a  $p$ -value  $> 0.1$  were removed from the model sequentially.

169 The final model was tested for multi-collinearity (variance inflation factor  $> 3$ ), normality,  
170 heteroscedasticity, high-leverage points or outliers (Cook's Distance  $> 1$ ) and spatial  
171 autocorrelation (using Moran's  $I$ ) of the residuals (Brunekreef, 2008). The model was validated  
172 using two approaches that are suitable for a small sample size (Dirgawati et al., 2015; Tang et



173 al., 2013). First, we used the ‘leave-one-out cross-validation’ (LOOCV) method, where the  
174 final model was fitted to  $N - 1$  sites and the predicted concentrations were compared to the  
175 measured concentration at the left-out site. As the LOOCV tends to overestimate the model  
176 performance, we also used the grouped cross-validation, where a random proportion (30%) of  
177 the data was used to train a model while the remainder was used for the prediction. This process  
178 was repeated 20 times and the average performance was used. The model performance was  
179 assessed using the  $R^2$ , the root mean square error (RMSE) and the mean squared error (MSE)–  
180  $R^2$ . The MSE- $R^2$  is a more representative metric to assess the goodness of fit around the 1:1  
181 line (Tang et al., 2013) and was calculated as:

182

$$183 \text{ MSE} - R^2 = 1 - \frac{\text{MSE}}{\left(\frac{1}{N} \sum_{i=1}^N (y_i - \bar{y}_t)^2\right)}$$

184

185 where  $y_i$  is the monitored NO<sub>2</sub> concentration at each site and  $\bar{y}_t$  the averaged NO<sub>2</sub>  
186 concentrations (Tang et al., 2013). Finally, the model results were mapped, with the study area  
187 divided into 50 m grid squares and NO<sub>2</sub> concentrations predicted for the centre of each grid  
188 square using the LUR model. Inverse distance weighting (IDW) was then used to interpolate  
189 the modelled NO<sub>2</sub> concentrations (Ghassoun et al., 2015; Liu et al., 2016). Analysis was done  
190 using R (3.2.4) and ArcGIS (v.10.2.2).

191

## 192 Model transferability

193 Model transferability was tested by transferring the model developed at the microscale to the  
194 local scale and city scale dataset collected during a previous study (Miskell et al., 2015). In  
195 addition, we applied the multi-scale (city and local scale) model developed by Miskell et al.  
196 (2015) to the Dominion Road dataset allowing coefficients to be flexible to explore the

197 potential to extend the multi-scale model to the microscale outside Auckland's CBD. A detailed  
198 description of the multi-scale model development is provided by Miskell et al. (2015). In brief,  
199 Miskell et al. (2015) developed a strategy to identify those predictor variables that were able  
200 to explain spatial variability of NO<sub>2</sub> at different spatial scales so that transferability of the model  
201 to either different locations or different scales may be improved. First, two LURs were  
202 developed at two different spatial scales (using the local scale and city scale data, Fig. 1)  
203 following the standard protocol. Next, these models were used on the other set of data (e.g.  
204 local scale model on the city scale data) in order to identify and remove any variables that may  
205 be present due to specifics of the data or due to model fitting (e.g. change in slope direction).  
206 The local scale model was then used on the city scale data, in order to improve the small-scale  
207 explanations, and the city scale model mostly used the local scale predictors. Following the  
208 model revision, those variables with *p*-values > 0.2 were removed, one at a time, to reach a  
209 new, revised model, which is referred to as the multi-scale model. This model had adjustable  
210 coefficient values for the different spatial scales in order to maximize specific fits and to give  
211 comparable performance results to those from their specific LUR models. This illustrated the  
212 potential to improve local scale explanations, with a requirement to validate this on a third,  
213 independent dataset.

214

## 215 Results and Discussion

### 216 Air pollution levels

217 A summary of NO<sub>2</sub> concentrations measured during each campaign and averaged over the  
218 whole study period (summer average) is shown in Table 2. In total, we made 149 measurements  
219 at the 40 sites, with some tubes lost or moved during each campaign. Overall, 32 sites had NO<sub>2</sub>  
220 concentrations from all campaigns, while the remaining sites were missing NO<sub>2</sub> concentration  
221 measurements for one (5 sites) or two campaigns (3 sites). The lower NO<sub>2</sub> concentrations

222 measured during campaign 4 are likely related to the lower traffic due to summer holidays. The  
 223 duplicates generally agreed well with an average (SD) CoV of 0.052 (0.053) and no sample  
 224 exceeded the threshold of 0.25. Mean NO<sub>2</sub> concentrations measured along Dominion Road  
 225 (overall 22 µg m<sup>-3</sup>) were below concentrations measured in North American and European  
 226 cities reviewed by Hoek et al. (2008), but similar or above concentrations measured during the  
 227 ESCAPE study in some European cities (e.g. Oslo, Norway (23 µg m<sup>-3</sup>), Copenhagen,  
 228 Denmark (18 µg m<sup>-3</sup>)) (Beelen et al., 2013) and above concentrations observed in streets in  
 229 Perth, Australia (12 µg m<sup>-3</sup>) (Dirgawati et al., 2015). The average was below that measured in  
 230 Auckland's CBD (34 µg m<sup>-3</sup>), where tall buildings and high bus traffic favour the build-up of  
 231 pollutants (Miskell et al., 2015; Weissert et al., 2015). Given that studies typically represent  
 232 annual averages, differences may partly be explained by temporal differences of the  
 233 measurements as we decided to present a seasonal average representative of summer, when  
 234 NO<sub>2</sub> concentrations are generally expected to be below the annual average. As expected, higher  
 235 concentrations were observed at sites around intersections while lower concentrations were  
 236 observed in park areas or streets away from the main road (Fig. 2).

237

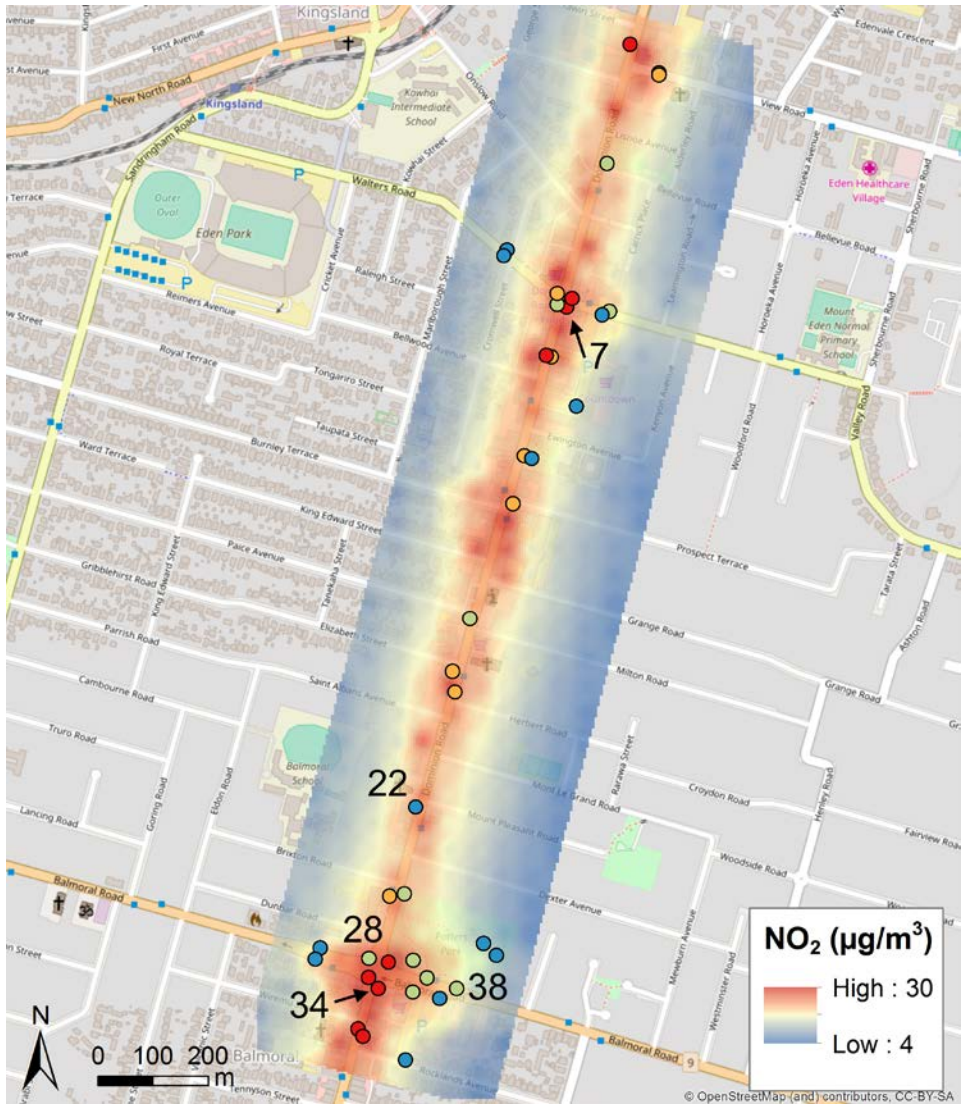
238 Table 2. Descriptive statistics of the NO<sub>2</sub> concentrations measured during summer 2016/2017  
 239 along Dominion Road (units are in µg m<sup>-3</sup>).

Sampling campaign	<i>n</i> (measurements)	Mean	Standard Deviation (SD)	Median	Min	Max	Range
1	35	23	7	22	12	34	22
2	39	21	6	22	12	35	23
3	36	27	7	26	15	42	27
4	39	16	6	17	7	28	21

Overall	40	22	6	22	12	34	22
---------	----	----	---	----	----	----	----

240

241



242

243 Fig. 2 NO<sub>2</sub> concentrations measured at the 40 sites (represented by the dots, with numbered  
 244 dots showing sites with largest discrepancies between modelled and measured NO<sub>2</sub>  
 245 concentrations) and modelled along Dominion Road.

246

247 Predictor variables

248 The predictor variables used in the final model were distance to major road, number of bus  
 249 stops within a 100 m buffer, presence of awnings and street width (Table 3). Of these, presence

250 of awnings (dispersion determinants) had the highest proportional contribution ( $\beta * (90^{\text{th}}$   
251 percentile –  $10^{\text{th}}$  percentile)) to the modelled NO<sub>2</sub> concentrations (79.08%), followed by  
252 number of bus stops within a 100 m buffer (16.52%) (Table 3). Distance to major road or street  
253 width only had a minor influence on modelled NO<sub>2</sub> concentrations. When comparing the  
254 predictor variables with city or regional scale LUR models (e.g. Beelen et al., 2013; Hoek et  
255 al., 2008), where predictor variables are usually related to traffic and land cover, it becomes  
256 evident that local scale street and building configurations become also important at the  
257 microscale. It is interesting to note that similar variables were also observed to be important in  
258 a local scale model in Auckland's CBD (e.g. number of bus stops, presence of awnings)  
259 (Miskell et al., 2015). Likewise, Tang et al. (2013) showed that including building and street  
260 configurations can be used to account for pollution dispersion and accumulation patterns in  
261 urban areas and improve the performance of LUR models. Following the ESCAPE protocol  
262 we removed two predictor variables from the model development (distance to tree, number of  
263 carparks) as they did not follow the expected pattern or slope of effect. In this study 'distance  
264 to tree' was not a significant variable in the model. This may be because trees can both act to  
265 increase and decrease air pollution concentrations depending on the dominant process. The  
266 presence of trees may improve air quality through enhanced deposition processes but trees may  
267 also decrease the dispersion of pollutants resulting in a local increase of NO<sub>2</sub> concentrations  
268 (Janhäll, 2015; Salmond et al., 2013). We also removed 'number of carparks' from the model  
269 because the effect of this parameter was variable depending on buffer size.

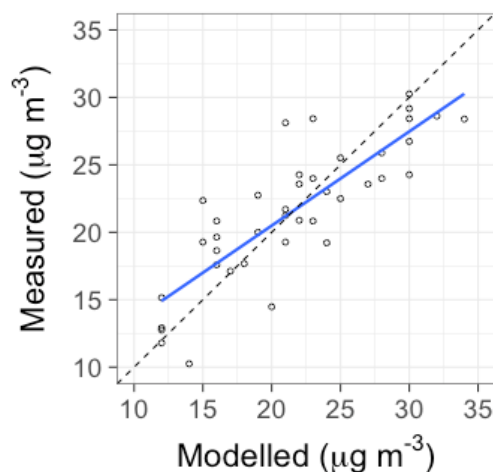
270

#### 271 LUR model results and limitations

272 The final model explained 66% of the variability in NO<sub>2</sub> concentrations with a RMSE of 3.317  
273  $\mu\text{g m}^{-3}$  (Table 3). On average, the modelled NO<sub>2</sub> concentrations were the same as the measured  
274 NO<sub>2</sub> concentrations with an almost equal number of over- and underestimated sites (18 and 17

275 sites, respectively). The largest difference between measured and modelled NO<sub>2</sub> concentrations  
276 were observed at site 22 and 28 where modelled NO<sub>2</sub> concentrations were 7 µg m<sup>-3</sup> above  
277 measured NO<sub>2</sub> concentrations. Observations at both sites were unexpectedly low given their  
278 location adjacent to Dominion road and close proximity bus stops. A further measurement  
279 campaign may be required to account for the discrepancy at these sites. In contrast, modelled  
280 NO<sub>2</sub> concentrations at sites 34, 38 and 7 were 6 µg m<sup>-3</sup> lower than those measured (Fig. 2).  
281 Again, the observed measurements at these sites were unexpected. Site 7 and 34 had higher  
282 measured NO<sub>2</sub> concentrations than sites in their surroundings with similar land use  
283 characteristics. Site 38 is located relatively far away from Dominion road, but is still located  
284 along a busy road, but this road is not accounted for in the model.

285 The  $R^2$  (MSE- $R^2$ ) and RMSE of the LOOCV validation were 0.60 (0.61) and 3.839 µg m<sup>-3</sup>,  
286 respectively (Table 4). A slightly lower MSE- $R^2$  (0.60) was achieved from the LGOCV method  
287 (Table 4). Nevertheless, both  $R^2$  are similar to the model  $R^2$  (Table 3) indicating that the model  
288 performed well under internal validation. The adjusted  $R^2$  is within the range of those achieved  
289 by LUR in European cities (55% - 92%) (Beelen et al., 2013). The RMSE, on the other hand,  
290 was lower than the RMSE of most cities in the ESCAPE study (Beelen et al., 2013), indicating  
291 a better overall accuracy of the LUR model due to data being less spread around the best-fit  
292 line.



293

294 Fig. 3 Modelled vs. measured NO<sub>2</sub> concentrations. The blue solid line represents the best-fit  
 295 and the dashed line shows the 1:1 line.

296

297 The diagnostic tests conformed to the requirements for regression analyses, with VIF's below  
 298 3 (Table 3), and no high-leverage points or outliers (max. Cook's D = 0.27) observed. The  
 299 Moran's *I* showed no spatial autocorrelation between the residuals ( $p = 0.915$ ). NO<sub>2</sub>  
 300 concentrations, as well as the residuals, were normally distributed (Shapiro Wilk,  $p > 0.05$ ).  
 301 The mapped NO<sub>2</sub> concentrations indicate high NO<sub>2</sub> concentrations underneath building  
 302 awnings, which may explain the higher concentrations visible adjacent to the road rather than  
 303 on the road. The presence of awnings combined with the density of bus stops also likely  
 304 explains the spatial variability in NO<sub>2</sub> concentrations along Dominion Rd (Fig. 2).

305

306 Table 3. Final LUR model.

LUR model	$\beta$	Std. Error	<i>p</i> -value	VIF	Proportional contribution <sup>1)</sup> (%)
Intercept	17.210	2.131	< 0.01		
Distance to major road	-0.055	0.013	< 0.01	1.57	0.78
Nr. of bus stops within a 100 m buffer	1.400	0.687	0.056	1.44	16.52
Awnings	5.436	1.815	< 0.01	1.15	79.08
Street width	0.248	0.075	< 0.01	1.04	3.61
Adj. $R^2$	0.66				
$R^2$	0.70				
RMSE ( $\mu\text{g m}^{-3}$ )	3.317				
MSE- $R^2$	0.71				

307 <sup>1)</sup>  $\beta$  \* (90<sup>th</sup> percentile – 10<sup>th</sup> percentile)

308

309 Table 4. Cross-validation results.

310

Validation method <sup>1)</sup>	RMSE	$R^2$	MSE	MSE- $R^2$	Iterations
LOOCV	3.839	0.60	14.738	0.61	-
LGOCV	3.886	0.65	15.101	0.60	20

311  
312  
313  
314

<sup>1)</sup> LOOCV = Leave-one-out cross-validation; LGOCV = grouped (leave-30%-out) cross-validation.

315 A limitation of the LUR model presented here, and microscale models in general, is the  
316 availability of traffic data at sufficient spatial and temporal scale. Google Maps traffic  
317 information only gives information about the typical traffic flow and is categorised into only  
318 four categories. Given the high spatial variability of air pollutants at the microscale future  
319 studies should also test the accuracy of the modelled NO<sub>2</sub> concentrations mapped in Fig. 2 and  
320 how these agree with exposure measurements.

321

#### 322 Within-city transferability of LUR models

323 The model developed in this study had relatively good performance when scaled up and  
324 applied to data previously reported at local and city scales in Auckland's CBD (Miskell et al.,  
325 2015), with an adjusted  $R^2$  of 0.57 and 0.76 and a Spearman rank correlation of 0.68 and 0.89,  
326 respectively (Table 5). Interestingly, the model performed better at the city scale, which was  
327 also the case when insignificant ( $p$ -value > 0.1) predictor variables (all except number of bus  
328 stops within 100 m) were removed (adj.  $R^2$  = 0.76, RMSE = 2.89). A slightly lower adjusted  
329  $R^2$  and Spearman rank correlation (0.68) was obtained when the microscale model was applied  
330 to the local scale dataset in the CBD, but apart from street width all predictor variables were  
331 significant (Table 5). If street width were removed following the ESCAPE protocol, the  
332 adjusted  $R^2$  was 0.54 and the RMSE was 3.891. This suggests that unlike standard LUR models  
333 which often perform poorly when applied to different areas of the city or scaled down, the



334 microscale variant developed here has reasonably good transferability in terms of both space  
335 and scale.

336 The multi-scale model presented by Miskell et al. (2015) also showed poor results when scaled  
337 down to microscales and applied to the data collected in this study. It could only explain 35%  
338 of the variability in NO<sub>2</sub> concentrations along Dominion Road, and distance to traffic light was  
339 not a significant predictor ( $p$ -value > 0.1) (Table 5). Thus, although the multi-scale model  
340 performed well for areas within the CBD it was not able to capture the variability of NO<sub>2</sub>  
341 concentrations outside the CBD where building and road configurations can be different (less  
342 and wider spaced traffic lights, lower buildings, etc.). What is interesting to note is that the  
343 only variable that was relevant in the multiscale model at all scales within and outside the CBD  
344 is the number of bus stops within 100 m. In Auckland, buses are almost exclusively run by  
345 diesel, which is the main source of NO<sub>2</sub> in Auckland. At smaller spatial scales (local and  
346 microscale) dispersion variables, such as presence of awnings, also becomes relevant.

347

348 Table 5. External validation of the Dominion Road LUR model and performance of multi-  
349 scale (local/city scale) model applied at different scales (Miskell et al., 2015). (Attached at  
350 the end of the manuscript)

351

## 352 Implications

353 The findings from this study have important implications for urban development indicating the  
354 importance of considering street and building configuration to minimize individual exposure  
355 to traffic related air pollutants. This might involve limiting the use of awnings near busy roads  
356 or developing pedestrian areas and walkways away from multi-lane roads. The strong influence  
357 of bus stops on NO<sub>2</sub> concentrations also supports the need to introduce electric and hybrid  
358 buses, which will be trialled in Auckland in 2017 (Auckland Council, 2017). A recent study in

359 Singapore also identified bus stops as hotspots of individual exposure and suggested to set bus  
360 shelters further away from the major road (Velasco and Tan, 2016). The results further indicate  
361 that models developed at city scales may not be able to capture the small scale variability in  
362 NO<sub>2</sub> concentrations along the road and that there is a need to consider dispersion features such  
363 as presence of awnings, supporting previous findings by Tang et al. (2013). The advantage of  
364 microscale models as presented in this study is the potential of estimating individual or  
365 population exposure at urban hotspots. These results may be used to assess differences in  
366 exposure depending on which side of the street pedestrians are walking on or to identify route  
367 choices with minimal exposure to traffic related air pollutants. Such detail is generally not  
368 available from LUR models developed at city or regional scales, which are commonly used to  
369 estimate individual exposure based on the residential address (Jerrett et al., 2007; Urman et al.,  
370 2014).

371 While the model developed at the microscale performed relatively well when transferred to  
372 different spatial scales in the city, it showed that the importance of predictor variables changes  
373 depending on location and spatial scale, limiting within-city transferability. Thus, as has been  
374 suggested by previous studies (Allen et al., 2011; Marcon et al., 2015; Vienneau et al., 2010),  
375 LUR models provide better results when developed locally and caution is required when  
376 transferring LUR models, even within cities, unless street and building configurations are  
377 similar. This also has some important implications for air quality monitoring, suggesting that  
378 future research should focus on monitoring NO<sub>2</sub> concentrations at a high spatial resolution  
379 within urban environments in order to obtain representative small-scale variability of pollutant  
380 concentrations at urban hotspots.

381

382 Conclusions

383 In this study, we assessed the performance of LUR modelling at the microscale representative  
384 of a busy street in Auckland, New Zealand. We showed that NO<sub>2</sub> concentrations can be  
385 modelled at this scale with a good performance of the model (adj.  $R^2 = 0.66$ , RMSE = 3.317 μg  
386 m<sup>-3</sup>). Unlike LUR models developed at the city or regional scale, this study has shown that  
387 building and street configuration, such as presence of awnings, is important predictors for NO<sub>2</sub>  
388 concentrations at the street level. The microscale model performed well when transferred to  
389 the city and local scale within Auckland's CBD, although the only significant predictor  
390 variables at all spatial scales was the number of bus stops within 100 m. The study indicated  
391 implications related to urban development, exposure assessments at urban hotspots and air  
392 quality monitoring, highlighting the importance of high density measurements or micro and  
393 local scale models to capture the small scale variability in NO<sub>2</sub> concentrations.

394

#### 395 Acknowledgments

396 The authors thank Auckland Council for providing the air quality data obtained from the  
397 routine monitoring network. We also thank Auckland Transport for permission to use lamp-  
398 posts for tube installation along Dominion Road and Alana Chester for helping with the  
399 laboratory analysis and preparation of figures.

400

#### 401 References

- 402 AEA Energy and Environment, 2008. Diffusion tubes for ambient NO<sub>2</sub> monitoring: Practical  
403 guidance for laboratories and users (Report to DEFRA and the Devolved  
404 Administrations), Didcot, UK.
- 405 Allen, R.W., Amram, O., Wheeler, A.J., Brauer, M., 2011. The transferability of NO and  
406 NO<sub>2</sub> land use regression models between cities and pollutants. Atmospheric  
407 Environment 45, 369 - 378.

408 Amini, H., Taghavi-Shahri, S.M., Henderson, S.B., Hosseini, V., Hassankhany, H., Naderi,  
409 M., Ahadi, S., Schindler, C., Kunzli, N., Yunesian, M., 2016. Annual and seasonal  
410 spatial models for nitrogen oxides in Tehran, Iran. *Sci Rep* 6, 32970.

411 Apte, J.S., Messier, K.P., Gani, S., Brauer, M., Kirchstetter, T.W., Lunden, M.M., Marshall,  
412 J.D., Portier, C.J., Vermeulen, R.C.H., Hamburg, S.P., 2017. High-Resolution Air  
413 Pollution Mapping with Google Street View Cars: Exploiting Big Data. *Environ Sci*  
414 *Technol.*

415 Auckland Council, 2017. Auckland Transport to trial electric buses.

416 Auckland Transport, 2017. Dominion Road upgrade.

417 Beelen, R., Hoek, G., Vienneau, D., ... , Brunekreef, B., de Hoogh, K., 2013. Development of  
418 NO<sub>2</sub> and NO<sub>x</sub> land use regression models for estimating air pollution exposure in 36  
419 study areas in Europe – The ESCAPE project. *Atmospheric Environment* 72, 10-23.

420 Borge, R., Narros, A., Artinano, B., Yagüe, C., Gomez-Moreno, F.J., de la Paz, D., Roman-  
421 Cascon, C., Diaz, E., Maqueda, G., Sastre, M., Quaassdorff, C., Dimitroulopoulou, C.,  
422 Vardoulakis, S., 2016. Assessment of microscale spatio-temporal variation of air  
423 pollution at an urban hotspot in Madrid (Spain) through an extensive field campaign.  
424 *Atmospheric Environment* 140 432 - 445.

425 Briggs, D.J., de Hoogh, C., Gulliver, J., Wills, J., Elliott, P., Kingham, S., Smallbone, K.,  
426 2000. A regression-based method for mapping traffic-related air pollution: application  
427 and testing in four contrasting urban environments. *The Science of the Total*  
428 *Environment* 253, 151 - 167.

429 Brunekreef, B., 2008. ESCAPE Study Manual, in: Institute of Risk Assessment Sciences,  
430 U.U. (Ed.), The Netherlands.

431 Chappell, P.R., 2014. The Climate and Weather of Auckland, in: NIWA (Ed.), 2 ed.

432 Dirks, K.N., Sharma, P., Salmond, J.A., Costello, S.B., 2012. Personal concentration to

433 air pollution for various modes of transport in Auckland, New Zealand. Open  
434 Atmospheric Science Journal 6, 84-92.  
435  
436 Dirgawati, M., Barnes, R., Wheeler, A.J., Arnold, A.-L., McCaul, K.A., Stuart, A.L., Blake,  
437 D., Hinwood, A., Yeap, B.B., Heyworth, J.S., 2015. Development of Land Use  
438 Regression models for predicting exposure to NO<sub>2</sub> and NO<sub>x</sub> in Metropolitan Perth,  
439 Western Australia. Environmental Modelling & Software 74, 258-267.  
440 Eeftens, M., Beekhuizen, J., Beelen, R., Wang, M., Vermeulen, R., Brunekreef, B., Huss, A.,  
441 Hoek, G., 2013. Quantifying urban street configuration for improvements in air  
442 pollution models. Atmospheric Environment 72, 1 - 9.  
443 Ghassoun, Y., Ruths, M., Lowner, M.O., Weber, S., 2015. Intra-urban variation of ultrafine  
444 particles as evaluated by process related land use and pollutant driven regression  
445 modelling. Sci Total Environ 536, 150-160.  
446 Grange, S.K., Dirks, K.N., Costello, S.B., Salmond, J.A., 2014. Cycleways and footpaths:  
447 What separation is needed for equivalent air pollution dose between travel modes?  
448 Transportation Research Part D: Transport and Environment 32, 111-119.  
449 Gurung, A., Levy, J.I., Bell, M.L., 2017. Modeling the intraurban variation in nitrogen  
450 dioxide in urban areas in Kathmandu Valley, Nepal. Environ Res 155, 42-48.  
451 Hoek, G., Beelen, R., de Hoogh, K., Vienneau, D., Gulliver, J., Fischer, P., Briggs, D., 2008.  
452 A review of land-use regression models to assess spatial variation of outdoor air  
453 pollution Atmospheric Environment 42, 7561 - 7578.  
454 Janhäll, S., 2015. Review on urban vegetation and particle air pollution - deposition and  
455 dispersion. Atmospheric Environment, 130 - 137.  
456 Jerrett, M., Arain, A., Kanaroglou, P., Beckerman, B., Potoglou, D., Sahuvaroglu, T.,  
457 Morrison, J., Giovis, C., 2005. A review and evaluation of intraurban air pollution  
458 exposure models. J Expo Anal Environ Epidemiol 15, 185-204.

459 Jerrett, M., Arain, M.A., Kanaroglou, P., Beckerman, B., Crouse, D., Gilbert, N.L., Brook,  
460 J.R., Finkelstein, N., Finkelstein, M.M., 2007. Modeling the intraurban variability of  
461 ambient traffic pollution in Toronto, Canada. *J Toxicol Environ Health A* 70, 200-  
462 212.

463 Kaur, S., Nieuwenhuijsen, M.J., 2009. Determinants of personal concentration to  
464 PM<sub>2.5</sub>, ultrafine particle counts, and CO in a transport microenvironment. *Environ.*  
465 *Science Technology* 43, 4737-4743.

466 Liu, C., Henderson, B.H., Wang, D., Yang, X., Peng, Z.R., 2016. A land use regression  
467 application into assessing spatial variation of intra-urban fine particulate matter  
468 (PM<sub>2.5</sub>) and nitrogen dioxide (NO<sub>2</sub>) concentrations in City of Shanghai, China. *Sci*  
469 *Total Environ* 565, 607-615.

470 Marcon, A., de Hoogh, K., Gulliver, J., Beelen, R., Hansell, A.L., 2015. Development and  
471 transferability of a nitrogen dioxide land use regression model within the Veneto  
472 region of Italy. *Atmospheric Environment* 122, 696 - 704.

473 McNabola, A., Broderick, B.M., Gill, L.W., 2009. A principal components analysis of the  
474 factors effecting personal concentration to air pollution in urban commuters in  
475 Dublin, Ireland. *J. Environ. Sci. Health* 44, 12, 1219-1226.

476 Meng, X., Chen, L., Cai, J., Zou, B., Wu, C.F., Fu, Q., Zhang, Y., Liu, Y., Kan, H., 2015. A  
477 land use regression model for estimating the NO<sub>2</sub> concentration in Shanghai, China.  
478 *Environ Res* 137, 308-315.

479 Miskell, G., 2013. Identifying urban design details affecting the spatial variability of micro-  
480 scale ambient nitrogen dioxide for the Auckland CBD area, School of Environment.  
481 University of Auckland, Auckland, NZ.

482 Miskell, G., Salmond, J., Longley, I., Dirks, K.N., 2015. A Novel Approach in Quantifying  
483 the Effect of Urban Design Features on Local-Scale Air Pollution in Central Urban

484 Areas. Environ Sci Technol 49, 9004-9011.

485 Mölter, A., Sindley, S., de Vocht, F., Agius, R., Kerry, G., Johnson, K., Ashmore, M., Terry,  
486 A., Dimitroulopoulou, S., Simpson, A., 2012. Performance of a microenvironmental  
487 model for estimating personal NO<sub>2</sub> exposure in children. Atmospheric Environment  
488 51, 225 - 233.

489 Morgenstern, V., Zutavern, A., Cyrys, J., Brockow, I., Gehring, U., Koletzko, S., Bauer, C.P.,  
490 Reinhardt, D., Wichmann, H.E., Heinrich, J., 2007. Respiratory health and individual  
491 estimated exposure to traffic-related air pollutants in a cohort of young children.  
492 Occup Environ Med 64, 8-16.

493 Salmond, J.A., McKendry, I.G., 2009. Chapter 2 Influences of Meteorology on Air Pollution  
494 Concentrations and Processes in Urban Areas, Air Quality in Urban Environments.  
495 The Royal Society of Chemistry, pp. 23-41.

496 Salmond, J.A., Williams, D.E., Laing, G., Kingham, S., Dirks, K., Longley, I., Henshaw,  
497 G.S., 2013. The influence of vegetation on the horizontal and vertical distribution of  
498 pollutants in a street canyon. Sci Total Environ 443, 287-298.

499 Senaratne, I., Shooter, D., 2004. Elemental composition in source identification of brown  
500 haze in Auckland, New Zealand. Atmospheric Environment 38, 3049-3059.

501 Shi, Y., Lau, K.K., Ng, E., 2016. Developing Street-Level PM<sub>2.5</sub> and PM<sub>10</sub> Land Use  
502 Regression Models in High-Density Hong Kong with Urban Morphological Factors.  
503 Environ Sci Technol 50, 8178-8187.

504 Statistics New Zealand, 2013. 2013 census usually resident population counts.

505 Stedman, J.R., Vincent, K.J., Campbell, G.W., Goodwin, J.W.L., Downing, C.E.H., 1997.  
506 New high resolution maps of estimated background ambient NO<sub>x</sub> and NO<sub>2</sub>  
507 concentrations in the UK. Atmospheric Environment 31, 3591 - 3602.

508 Tang, R., Blangiardo, M., Gulliver, J., 2013. Using building heights and street configuration

509 to enhance intraurban PM<sub>10</sub>, NO(x), and NO<sub>2</sub> land use regression models. Environ  
510 Sci Technol 47, 11643-11650.

511 Urman, R., McConnell, R., Islam, T., Avol, E.L., Lurmann, F.W., Vora, H., Linn, W.S.,  
512 Rappaport, E.B., Gilliland, F.D., Gauderman, W.J., 2014. Associations of children's  
513 lung function with ambient air pollution: joint effects of regional and near-roadway  
514 pollutants. Thorax 69, 540-547.

515 Vardoulakis, S., Solazzo, E., Lumberras, J., 2011. Intra-urban and street scale variability of  
516 BTEX, NO<sub>2</sub> and O<sub>3</sub> in Birmingham, UK: Implications for exposure assessment.  
517 Atmospheric Environment 45, 5069-5078.

518 Velasco, E., Tan, S.H., 2016. Particles exposure while sitting at bus stops of hot and humid  
519 Singapore. Atmospheric Environment 142, 251-263.

520 Vienneau, D., de Hoogh, K., Beelen, R., Fischer, P., Hoek, G., Briggs, D., 2010. Comparison  
521 of land-use regression models between Great Britain and the Netherlands.  
522 Atmospheric Environment 44, 688 - 696.

523 Weissert, L.F., Salmond, J., Friedel, A., LaFave, M., Schwendenmann, L., 2015. Temporal  
524 and spatial patterns of carbon dioxide mixing ratios in a subtropical urban  
525 environment during spring. Weather and Climate 35, 13 - 32.

526 Xie, M., Zhu, K., Wang, T., Chen, P., Han, Y., Li, S., Zhuang, B., Shu, L., 2016. Temporal  
527 characterization and regional contribution to O and NO at an urban and a suburban  
528 site in Nanjing, China. Sci Total Environ 551-552, 533-545.



Table 1. Predictor variables used for the model development with defined buffer sizes, impact and expected direction of effect.

Variable	Variable description	Impact	Unit	Direction of effect	Buffer size radius (m)
Kerb length	Length of kerb within buffer size	Modifier	m	+	10, 25, 50, 100
Distance to traffic light	Distance to nearest traffic light	Source	m	-	NA
Distance to intersection	Distance to nearest intersection	Source	m	-	NA
Distance to major road	Distance to major road (including arterial roads going in and out of the city, major urban roads and motorways)	Source	m	-	NA
Height-width ratio	Height of surrounding buildings divided by street width	Modifier	ratio	+	NA
Car parks	Sum of large car parks within a buffer size	Source	count	+	25, 50, 100
Nr. of lanes	Sum of traffic lanes along nearest road	Source	count	+	NA
Distance to bus stop	Distance to nearest bus stop	Source	m	-	NA
Nr. of bus stops	Sum of bus stops within buffer size	Source	count	+	10, 25, 50, 100
Nr. of bus lanes	Sum of bus lanes within buffer size	Source	count	+	10, 25, 50, 100
Tree density	Tree density within buffer size	Source	Trees/m <sup>2</sup>	-	10, 25, 50, 100
Distance to tree	Distance to nearest tree	Modifier	m	+	NA
Vegetation	Presence of tree within buffer size	Modifier	Y = 1, N = 0	-	10, 25, 50, 100
Side of street	Left or right with a north/east orientation	Modifier	L = 1, R = 0	NA	NA
Street width	Distance from one side of the street to the other	Modifier	m	+	NA
Awnings	Presence of awnings within 10 m	Modifier	Y = 1, N = 0	+	NA
Building footprint	Area of buildings within a buffer size	Modifier	m	+	25, 50, 100
Morning rush hour traffic	Average traffic flow estimated from GoogleMaps during weekday morning rush hour	Source	1: Slowest, 4: Fastest	+	NA
Midday traffic	Average weekday traffic flow at midday estimated from GoogleMaps	Source	1: Slowest, 4: Fastest	+	NA
Evening rush hour traffic	Average traffic flow estimated from GoogleMaps during weekday evening rush hour	Source	1: Slowest, 4: Fastest	+	NA

Table 5. External validation of the micro scale Dominion Road LUR model and performance of multi-scale (local/city scale) model applied at different scales (Miskell et al., 2015). <sup>1)</sup>

Model	Dataset	Nr. Locations	Spatial scale	Variables <sup>1)</sup>	Adj. $R^2$	RMSE ( $\mu\text{g m}^{-3}$ )	Spearman rank correlation
Micro scale (Dominion Road)	Dominion Rd	40	Micro	Distance to major rd*** Nr. of bus stops within 100 m Awnings** Street width**	0.66	3.317	0.84
	CBD	62	Local	Distance to major rd* Nr. of bus stops within 100 m*** Awnings*** Street width	0.57	4.852	0.68
	CBD	21	City	Distance to major rd Nr. of bus stops within 100 m*** Awnings Street width**	0.76	2.758	0.89
Multi-scale (Miskell et al., 2015)	Dominion Rd	40	Micro	Nr. of lanes Nr. of bus stops within 100 m** Distance toward traffic light	0.35	4.647	0.59
	CBD	62	Local	Nr. of lanes*** Nr. of bus stops within 100 m*** Distance toward traffic light**	0.54	5.058	0.67
	CBD	21	City	Nr. of lanes*** Nr. of bus stops within 100 m*** Distance toward traffic light*	0.79	2.661	0.91

\*  $p$ -value < 0.1, \*\*  $p$ -value < 0.05, \*\*\*  $p$ -value < 0.01